

Supplementary Information

Improved visible light photocatalytic nitrogen fixation activity using a Fe^{II}-rich MIL-101(Fe): Breaking the scaling relationship by photoinduced Fe^{II}/Fe^{III} cycling

Lijun Guo ^{a,b,†}, Feifei Li ^{a,†}, Jianxin Liu ^{a*}, Zehui Jia ^a, Rui Li ^a, Zhuobin Yu^c, Yawen Wang ^a,
Caimei Fan ^{a*}

*a. College of Chemical Engineering and Technology, Taiyuan University of Technology,
Taiyuan 030024, PR China*

*b. Department of Chemistry and Chemical Engineering, Taiyuan Institute of
Technology, Taiyuan 030008, PR China*

*c. Instrumental Analysis Center of Taiyuan University of Technology, Taiyuan
University of Technology, Taiyuan 030024, PR China*

**Corresponding author : Caimei Fan (fancm@163.com) ;*

Jianxin Liu(liujx0519@163.com)

†These authors contributed equally to the work.

CONTENT

1. Supporting Experimental Section.....	S3
2. Characterization Methods	S4
3. Theoretical Calculations	S4
4. Supporting Data.....	S5
5. References	S9

1. Supporting Experimental Section

1.1 Electrochemical Measurements

The electrochemical experiments were conducted on a Squidstat Plus electrochemical workstation to characterize photoelectric current and the Mott-Schottky plots. A Pt plate and a standard Ag/AgCl electrode served as the counter and reference electrodes, respectively. The electrolyte used was a 0.5 M Na₂SO₄ aqueous solution.

1.2 Nitrogen-Reduction Apparent Quantum Efficiency Measurements

The experiments for determining AQE were performed in 50 mL ultrapure water in the same nitrogen fixation condition with different monochromatic filters (i.e., 420, 450, 500, 520, and 600 nm), and the irradiation area was 28.26 cm². 50 mg of as-synthesized catalysts were used as the photocatalysts, and the reaction time was 1 h. The average intensity of irradiation was measured to be 29.04, 28.24, 21.14, 15.66, and 19.9 mW cm⁻², respectively. The AQE was calculated from the following equation¹:

$$AQE = \frac{N_e}{N_p} = \frac{6N_{AM}}{N_p} = \frac{6n_{AM}N_A}{\frac{WAt}{h\nu}} \times 100\%$$

1.3 ¹⁵N₂ isotope labelling experiments

¹H NMR spectroscopy analysis was measured using AVANCEAV III 400 (Bruker, Germany). 5 mL reaction liquid was filtrated by a 0.22 μm membrane to remove solid catalysts. the obtained solution was adjusted by 6 mol L⁻¹ HCl solution to pH=1.2. Add 100 μL DMSO-d₆ to 500 μL acidized solution and mix adequately.

2. Characterization Methods

The crystalline phases of the samples were characterized by X-ray powder diffraction (XRD) instrument (Rigku, Japan) with the 2θ range of 5° to 80°. The surface compositions were analyzed using X-ray photoelectron spectroscopy (XPS, Thermo

Scientific ESCALAB 250Xi, USA). The morphologies of samples were observed by scanning electron microscopy (SEM, JSM-7200F, Japan). Fourier transform infrared spectroscopy (FTIR) spectra were recorded in the range of 400–4000 cm^{-1} using KBr pellets (Nicolet iS50, USA). The thermostability of the samples was characterized by Thermogravimetric (TGA, TG209 F3, Germany). UV–vis diffuse reflection spectra (DRS) was recorded on a UV-vis spectrophotometer (SU-3900, Japan). Inductively coupled plasma (ICP) was carried out with Varian 720 (Japan). Electron spin resonance (EPR, JES FA200, Japan) was utilized to detect iron species. Photoluminescence spectra (PL) were obtained on a Fluorescence Spectrophotometer (FLS980, UK) at room temperature. The in situ FTIR experiments were performed with Tensor II instrument (Bruker, Germany).

3. Theoretical Calculations

Density functional theory (DFT)² simulations computations were performed using the Vienna ab initio simulation package (VASP) software³ with the projector-augmented plane wave (PAW)⁴ to calculate the adsorption of N_2 . The generalized gradient approximation (GGA)⁵ was expressed by the Perdew, Burke, and Ernzerhof (PBE)⁶ functional. 450 eV cutoff energy for the planewave basis was set for all computations. The van der Waals interaction was described by using the semiempirical DFT-D3⁷ approach. The Brillouin zone was sampled by $1 \times 1 \times 1$ k-points within the Monkhorst-Pack scheme for structural optimization. We set the convergence criteria for energy and force to be 1×10^{-5} eV and 0.02 eV/Å, respectively.

4. Supporting Data

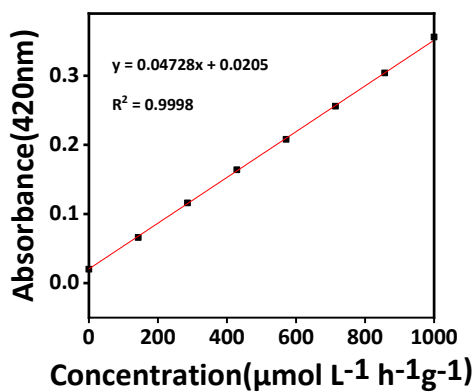


Fig. S1 UV-vis absorption spectra of ammonia standard curve for ammonia detection with Nessler's reagent

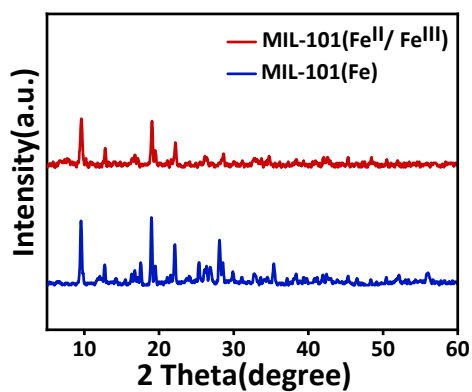


Fig.S2 XRD patterns of MIL-101(Fe^{II}/ Fe^{III}) and MIL-101(Fe) samples

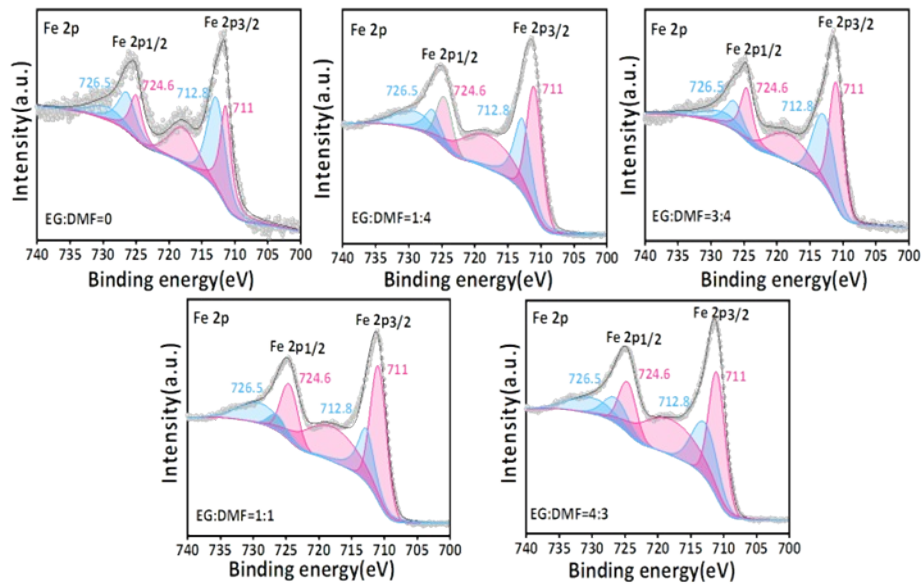


Fig.S3 Fe 2p XPS spectra of different EG dosage

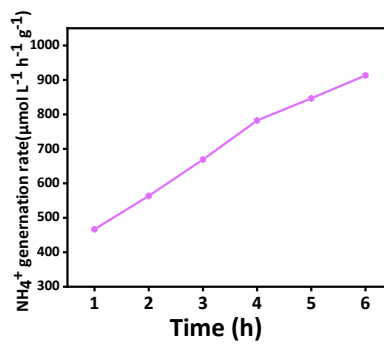


Fig.S4 NH₄⁺ generation rate of MIL-101(Fe^{II}/Fe^{III}) in the long-term photocatalytic experiments

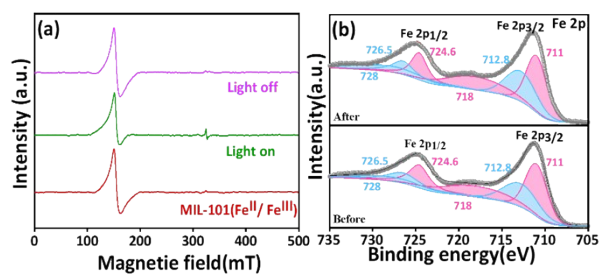


Fig.S5 (a) EPR spectra at different experimental stages, (b) Fe 2p XPS spectrum of MIL-101(Fe^{II}/Fe^{III}) after nitrogen fixation reaction

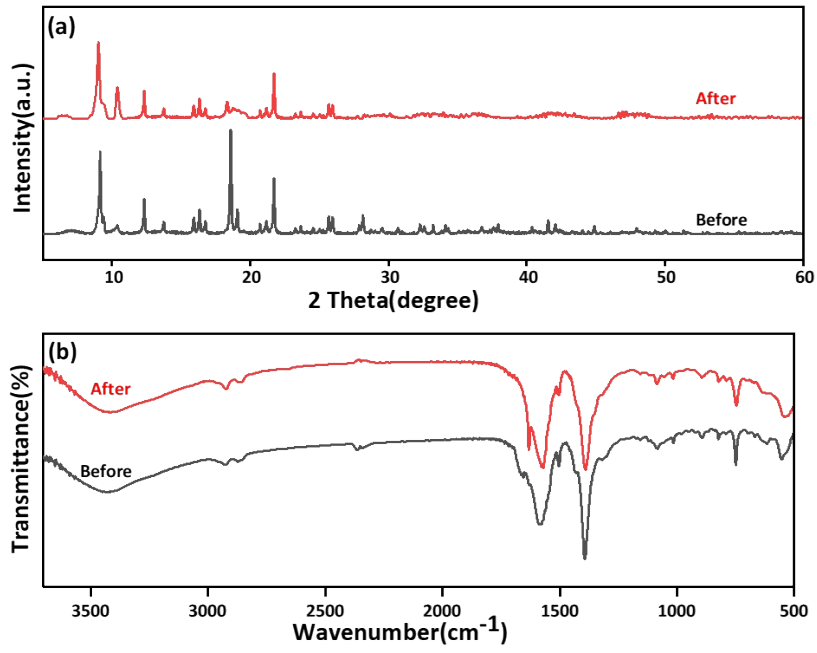


Fig.S6 (a) XRD pattern and (b) FTIR spectra of MIL-101(Fe^{II}/ Fe^{III}) before and after nitrogen fixation reaction

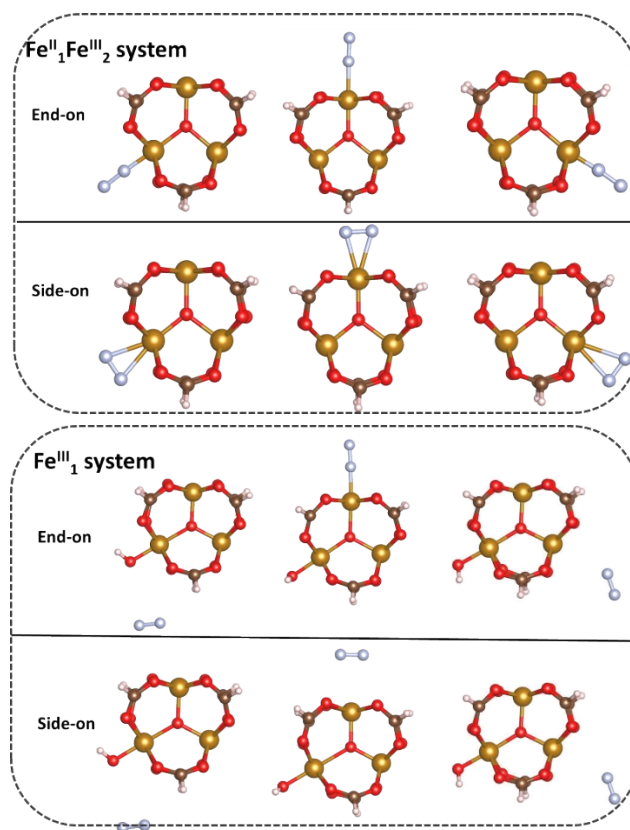


Fig.S7 The coordinated N₂ models of side-on and end-on in Fe^{II}₁Fe^{III}₂ system and Fe^{III}₃ system, respectively

Table S1 Catalyst performance of different EG dosage

EG: DMF	MIL-101(Fe)		MIL-101(Fe ^{II} /Fe ^{III})			
	0	1:4	3:4	1:1	4:3	4:1
NH ₄ ⁺ production rate(μmol h ⁻¹ g ⁻¹)	93.8	326.9	466.8	376	367	--
the ratio of Fe ^{II} /Fe ^{III}	0.8	1.24	1.4	1.47	1.4	--

Table S2 Specific values of AQE of MIL-101(Fe^{II}/Fe^{III}) and MIL-101(Fe)

Wavelength(nm)	420	450	500	520	600
MIL-101(Fe ^{II} /Fe ^{III})	0.52	0.22	0.11	0.07	0.024
MIL-101(Fe)	0.29	0.02	0	0	0

Table S3 Adsorption energy of different iron sites in Fe^{II}₁Fe^{III}₂ system and Fe^{III}₃ system

		Fe ^{II} ₁ Fe ^{III} ₂ system 1	Fe ^{II} ₁ Fe ^{III} ₂ system 2	Fe ^{II} ₁ Fe ^{III} ₂ system 3	Fe ^{III} ₃ system 1	Fe ^{III} ₃ system 2	Fe ^{III} ₃ system 3
Adsorption energy(eV)	End-on	-0.3272	-0.1973	-0.3409	-0.1761	-0.2327	-0.0054
	Side-on	0.18343	0.0042	0.0060	-0.1761	0.0186	-0.0054

5. References

1. N. Zhang, L. Li, Q. Shao, T. Zhu, X. Huang and X. Xiao, *ACS Appl. Energ. Mater.*, 2019, **2**, 8394-8398.
2. W. Tu, Y. Zhou and Z. Zou, *Adv. Mater.*, 2014, **26**, 4607-4626.
3. N. Armaroli and V. Balzani, *Chemistry*, 2016, **22**, 32-57.
4. D. Chen, X. Zhang and A. F. Lee, *J. Mater. Chem. A*, 2015, **3**, 14487-14516.
5. J. P. Perdew, K. Burke and Y. Wang, *Phys Rev B Condens Matter*, 1996, **54**, 16533-16539.
6. J. Wang, J. Sun, C. Hu, Z. Liu and S. Hu, *J. Electroanal. Chem.*, 2015, **759**, 2-7.
7. S. Grimme, J. Antony, S. Ehrlich and H. Krieg, *J. Chem. Phys.*, 2010, **132**, 154104.